Cancer Letters 452 (2019) 213–225

Contents lists available at ScienceDirect

Cancer Letters

journal homepage: www.elsevier.com/locate/canlet

Original Articles

Induction of breast cancer stem cells by M1 macrophages through Lin-28B-let-7-HMGA2 axis

Liang Guo[a,*,1], Xiang Cheng[a,1], Hongyu Chen[a], Changguo Chen[b], Shuai Xie[c], Min Zhao[a], Dan Liu[a], Que Deng[a], Yanjun Liu[c], Xiaomeng Wang[a], Xintian Chen[d], Jiangong Wang[d], Zhaoyang Yin[e], Siyong Qi[e], Jiangping Gao[e], Yuanfang Ma[c], Ning Guo[a], Ming Shi[a,**]

[a] Institute of Basic Medical Sciences, Beijing, 100850, PR China
[b] Department of Clinical Laboratory, The Navy General Hospital, Beijing, 100048, PR China
[c] Laboratory of Cellular and Molecular Immunology, Medical School of Henan University, Kaifeng, 475004, PR China
[d] Department of Cancer Biotherapy, Cancer Institute, Tangshan People's Hospital, Tangshan, 063001, PR China
[e] Department of Urology, The First Affiliated Hospital, General Hospital of PLA, Beijing, 100048, PR China

ARTICLE INFO

Keywords:
Cancer stem cell
Macrophage
Stat3
NF-κB
Lin-28B-let-7-HMGA2

ABSTRACT

Proinflammatory macrophage (M1) is now being suggested as a potential therapeutic strategy for cancer because of its tumoricidal capacity. However, few studies have been focused directly on the effects of M1 macrophages on cancer cells. Here, we found that M1 induced a subpopulation of $CD44^{high}/CD24^{-/low}$ or $ALDH1^{+}$ cells with CSC-like phenotypes from different types of breast cancer cells (BCCs) in a paracrine manner. Stat3/NF-κB pathways in BCCs were activated by proinflammatory cytokines, igniting Lin-28B-let-7-HMGA2 axis to induce CSC through epithelial-mesenchymal transition (EMT). Previously, we reported that Stat3-coordinated Lin-28B-let-7-HMGA2 axis initiated EMT in BCCs. Here, inhibition of Stat3/NF-κB pathways or Lin-28B-let-7-HMGA2 axis suppressed EMT/CSCs program. Notably, HMGA2 knockdown directly repressed M1-induced CSC formation and expression of Klf-4 and Nanog. Meanwhile, prolonged coculture with BCCs endowed M1 with M2 properties. M1 supernatant induced CSC from non-stem cancer cells, while M2 supernatant sustained a higher proportion of $ALDH1^{+}$ cells. Our data suggest that macrophages might modulate CSC formation and maintenance by transferring between M1/M2 phenotype. Given that M1 are being considered as a promising immunotherapy tool, it is important to inhibit their CSC-inducing potential by targeting key molecules and pathways.

1. Introduction

Macrophages have been demonstrated to be the most abundant immune cells in solid tumors, comprising 5–40% of tumor mass. In early tumors, macrophages appear to possess "classically activated" (M1) phenotype to play proinflammatory tumoricidal roles [1]. As tumors are established, macrophages tend to be educated by tumor cells towards immunosuppressive "alternatively activated" phenotype (M2) to aid tumor progression [2]. Mounting evidence suggests that an elevated number of TAMs with M2 profile is correlated with therapy failure and poor prognosis in patients [3–6], indicating TAM an important target in anti-tumor therapy [7,8]. Attempts have been made to increase M1/M2 ratio in tumors by inducing TAMs to switch from M2 to M1 or injecting polarized M1 into tumors [9–11], showing that increased M1 macrophages efficiently reduced tumor burden and malignancy in mouse models. Furthermore, modulation of TAMs is also required by other immunotherapies to succeed. Change of TAM phenotype to M1 augmented the anti-tumor efficacy of $CD8^{+}$ T cells in lung and melanoma cancers in vivo [12,13]. Monoclonal antibodies targeting programmed cell death protein-1 (α-PD-1) have shown notable clinical efficacy in patients with various cancer. However, $PD\text{-}1^{-}$ TAMs could capture α-PD-1 from T cell surface and dramatically reduce the efficacy of α-PD-1 in activating T cells [14]. These data suggest that modulating TAMs would be a promising cancer therapy and also beneficial for other established immunotherapies. Though M2 phenotype has been considered to be the major phenotype of TAM, TAMs with a mixed M1/M2 phenotype are also present in patients of pancreatic cancer, T cell/histiocyte rich large B cell lymphoma and ovarian cancer

* Corresponding author.
** Corresponding author.
E-mail addresses: gllsunmo369@sina.com (L. Guo), sm200@sohu.com (M. Shi).
[1] Contributed equally.

https://doi.org/10.1016/j.canlet.2019.03.032
Received 9 April 2018; Received in revised form 12 March 2019; Accepted 20 March 2019

[15–18]. In pancreatic ductal adenocarcinoma (PDAC) patients, TAMs exhibiting M1 phenotype were detected and both pro- and anti-inflammatory macrophages contributed equally to EMT in PDAC initiation and development [15]. Very recently, it has also been revealed that polarized M1 macrophages enhances the metastasis potential of ovarian cancer cell lines via NF-κB pathway [19]. These evidences indicate that the pro-inflammatory signals of tumor-associated macrophages might function in tumor progression, so strategies using M1 macrophages in cancer treatment should be regarded with some caution and more studies should be focused on the effect of M1 macrophages on cancer cells.

Cancer stem cells (CSCs) are a minority subpopulation of highly tumorigenic cells in tumors, which have been identified in a wide variety of cancers [20]. It has been suggested that CSCs may arise from non-stem cancer cells (NSCCs) upon microenvironment signals [21,22]. However, the mechanisms of CSC formation still remain elusive. Ablation of macrophages in mouse mammary fat pad severely impaired the function of stem/progenitor cells in developing mammary gland and almost completely blocked tumor initiation in mouse models, suggesting a critical correlation between macrophages and CSCs [23]. M2 TAMs have been indicated to support CSC signatures [24,25]. Both M1 and M2 TAMs are observed in tumor tissues and the transient activation status is essential for macrophages to acquire M2 phenotype. Also, pro-inflammatory cytokines such as interleukin (IL)-1β, IL-6, and IL-8 contributed to the establishment of CSC niche. Since CSCs are a major cause for tumor metastasis, drug resistance and relapse and M1 macrophages are being introduced into cancer treatments, it is worth investigating any potential correlation between macrophages and CSCs.

Accumulating evidence indicates that stem cell-like properties can be induced in cancer cells via epithelial-mesenchymal transition (EMT), during which epithelial cells lose their cell polarity and cell-cell adhesion and gain migratory and invasive properties. Previously, we reported that in breast cancer cells, Stat3-coordinated Lin-28B-let-7-HMGA2 axis effectively initiated EMT in response to inflammatory cytokine Oncostatin M (OSM) and inflammatory pathways IL-6/Stat3/Jagged-1/Notch could increase drug resistance of gastric cancer cells via EMT/CSC process [26,27].

In this study, we found that M1 macrophages contribute to the initiation of CSC phenotypic transformation in breast cancer cells. M1-associated inflammatory cytokine network triggers the expansion and self-renewal of CSCs through Lin-28B-let-7-HMGA2 axis. Our data also suggest that upon interplay with tumor cells, M1 transdifferentiate into M2 phenotype, which function in supporting CSC maintenance. This study not only sheds a new light on the potential mechanism of CSC generation, but more importantly, indicates that when M1 macrophage is utilized as a powerful tool to kill cancer cells, it is of great importance to suppress potential CSC formation and maintenance by blocking key pathways and preventing M1 from switching to M2 phenotype.

2. Material and methods

2.1. Cell culture

Human breast cancer cell lines MCF-7, T47D, BT474, and MDA231 were cultured in Dulbecco's Modified Eagle's Medium (DMEM, Invitrogen) supplemented with 10% fetal bovine serum (FBS) in a 5% CO_2 atmosphere at 37 °C. Human monocytic cell line THP-1 was cultured in RPMI 1640 medium supplemented with 10% FBS. Stable depletion of *HMGA2* in MDA-MB-231 cells was achieved by transfection of the HMGA2 shRNA expression vector and the transfected cells were maintained in DMEM containing 10% FBS and 400 ng/ml G418 (Invitrogen).

To analyze the activation of Stat3 and NF-κB signaling pathways, breast cancer cells were pre-treated with 50 μM Janus kinase 2 (JAK2) inhibitor AG490 (Sigma), 5 μM nuclear factor κB (NF-κB) inhibitor BAY11-7082 (InvivoGen) or both for 1 h and then cocultured with the proinflammatory macrophages.

To determine the effects of proinflammatory cytokines on the formation of CSCs, MCF-7 cells were treated with 50 ng/ml of IL-1β, IL-6, and TNF-α, respectively, or with all three cytokines for 24 h. THP-1-polarized proinflammatory macrophages were pre-treated with anti-IL-6 (0.5 μg/ml, PEPROTECH), anti-TNF-α (0.5 μg/ml, PEPROTECH), anti-IL-1β antibodies (2.5 μg/ml, eBioscience), respectively, or with all the three antibodies for 1 h and then co-cultured with MCF-7 cells for additional 24 h. Co-cultured MCF-7 cells were analyzed by flow cytometry and Western blot.

2.2. M1 and M2 macrophage polarization

The protocols of M1 and M2 macrophages polarization from THP-1 cells and human monocytes were adopted from Tjiu et al. [28]. Briefly, THP-1 cells were treated with 320 nM phorbol-12-myristate-13-acetate (PMA; Sigma) for 6 h and then with PMA plus 100 ng/ml lipopolysaccharide (LPS) (Sigma) and 20 ng/ml interferon-γ (IFN-γ; PEPROTECH) or 20 ng/ml IL-4 (PEPROTECH) and 20 ng/ml IL-13 (PEPROTECH) for 18 h to obtain the M1and M2 phenotype, respectively.

Human peripheral blood mononuclear cells (PBMC) were treated with 100 ng/ml macrophage colony-stimulating factor (M-CSF, PEPROTECH) in RPMI 1640 medium supplemented with 20% FBS for 6 d. To generate the M1 macrophages, the cells were treated with 100 ng/ml LPS and 20 ng/ml IFN-γ for an additional 72 h.

2.3. Co-culture of macrophages and breast cancer cells

1×10^6 THP-1 cells were seeded into the upper insert of a six-well transwell apparatus (0.4 μm pore size, BD Biosciences) and polarized into the M1 or M2 macrophages. After thoroughly washing to remove all PMA and cytokines, the THP-1-derived M1 or M2 macrophages were co-cultured with 3×10^5 MCF-7 breast cancer cells in six-well plates for indicated time points. Then the macrophages in upper inserts and breast cancer cells in six-well plates were used for subsequent experiments. The experiments were repeated at least twice.

2.4. Flow cytometry

Macrophages were washed and resuspended in phosphate buffered saline (PBS). The cells were then incubated with PE-conjugated anti-CD197 (eBioscience), anti-CD163 (eBioscience), or anti-CD206 (eBioscience) antibodies for 30 min in dark at room temperature. After washing with PBS twice, the labeled cells were analyzed on a FACScan flow cytometer using CellQuest software (BD Biosciences). The experiments were repeated at least twice.

MCF-7 cells were pre-treated by the supernatant of M1 macrophages (M1-S) for 24 h. CSCs were sorted by using ALDEFLUORTM kit (StemCell Technologies) according to the manufacturer's protocol. $ALDH1^+$ cells were plated at 2×10^5 cells per well in 6-well plates pre-coated with rat-tail collagen in DMEM/F12 containing 5% FBS and 25% supernatant of THP-1, M1-S, and M2-S and incubated for 4 d. NSCCs were seeded at 2×10^5 cells per well in 6-well plates and incubated in DMEM containing 10% FBS and 25% supernatant of THP-1, M1-S, and M2-S for 24 h. Then CSCs and NSCCs were analyzed by ALDEFLUOR-based FACS assay.

2.5. RNA extraction and real-time PCR

To determine the alterations of the cytokine mRNAs in breast cancer cells and macrophages, total RNAs were prepared using Trizol reagent from each sample and reverse transcribed using RevertAid First Strand cDNA Synthesis Kit (Fermentas). Real-time PCR was then carried out in a total of 20 μl reaction mixture using a Stratagene Mx3000P system with SYBR Mix (Thermo Fisher Technology). Data were then analyzed according to the comparative Ct method and normalized to GAPDH or

U6. The experiments were repeated at least twice. Primer sequences for real-time PCR were listed in supplemental legends.

2.6. Western blot

Western blotting was performed as previously described. Cell extracts were subjected to SDS-PAGE and transferred to a PVDF membrane. Immunoblot analysis was performed with antibodies against E-cadherin (Santa Cruz), fibronectin (Santa Cruz), Stat3 (Santa Cruz), p65 (Santa Cruz), p-Stat3 (Cell Signaling Technology), p-p65 (ImmunoWay), ZEB1 (ABclonal), HMGA2 (ABGENT), and Lin-28B (ABGENT), followed by horseradish peroxidase-conjugated secondary antibodies. Bands were visualized by the enhanced chemiluminescence assay (Thermo).

2.7. Transfection of miRNA mimics and siRNA

MCF-7 cells were seeded at 3×10^5 cells per well in 6-well plates and transfected with let-7 mimics at a final concentration of 50 nM using RNAiMAX (Invitrogen) according to the manufacturer's instructions. After 24 h of transfection, the cells were co-cultured with or without the proinflammatory macrophages for 24 h. To knockdown the expression of Stat3, p65, or HMGA2 in MCF-7 cells, 50 nM specific siRNAs were transfected into the cells. The experiments were repeated at least twice.

2.8. Luciferase reporter assay

Cells were seeded in 24-well plates in duplicate one day prior to transfection. Then the cells were co-transfected with 300 ng of Stat3 or NF-κB luciferase reporter plasmid and 30 ng pRL-TK reporter plasmid. After 24 h, the cells were treated with M1-S for the indicated time points. The luciferase activities were measured using the Dual-Luciferase Reporter Assay System (Promega) and normalized to Renilla luciferase activities. The experiments were repeated at least twice.

2.9. Immunofluorescence

3×105 cells were seeded in 35 mm dishes overnight, washed twice, and then treated with THP-1-S, M1-S, or M2-S for 24 h. The cells were fixed with 4% paraformaldehyde at 4 °C for 10 min followed by washing with PBS. After blocking with 3% BSA in PBS for 45 min at room temperature, the cells were incubated with the anti-fibronectin (Santa Cruz) and anti-E-cadherin antibodies (Santa Cruz) for 12 h at 4 °C. After washing with PBS twice, the cells were incubated with fluorescein-labeled secondary antibodies (Life Technologies, A11012& A11001) for 1 h at room temperature in dark. The cells were then washed twice, stained with DAPI (5 μg/ml) in PBS for 15 min, and observed under a laser scanning confocal microscope (Zeiss LSM510). Digital images were taken.

Breast cancer tissues were obtained from Hebei Hospital (Shijiazhuang, Hebei, China). Written informed consents were obtained from the patients for the use of the tumor tissue samples in this research. The study was approved by the Ethics and Scientific Committee of Hebei Hospital. Paraffin-embedded tissue sections were stained with the anti-NOS2 (Santa Cruz) and anti-ALDH1 (ABGENT) primary antibodies and fluorescein-labeled secondary antibodies. All the methods were performed in accordance with relevant guidelines and regulations.

2.10. In vitro cell invasion assay

Matrigel invasion assays were performed using a 24-well invasion chamber system with 8 μm pore polycarbonate membrane inserts (Costar) coated with Matrigel basement membrane matrix (BD Biosciences) on the top. Briefly, RPMI 1640 medium supplemented with 20% FBS was placed in the lower compartment of the chamber. 1×10^5 breast cancer cells in 200 μl of serum-free RPMI 1640 medium were seeded on the inserts. The cells that had migrated and invaded through the inserts were stained with crystal violet and photographed under an Olympus microscope. The uptaken crystal violet was solubilized in 33% acetic acid solution. The amount of dye was quantified by measuring the absorbance at 570 nm. The experiment was repeated twice.

2.11. Immunohistochemistry

Immunohistochemical staining was performed as previously described. The expression of Ki67 in MDA-MB-231 human breast cancer xenografts was detected by the rabbit polyclonal antibodies against Ki67 (Santa Cruz). Images were taken on an Olympus BX51 microscope using the Spot insight image capture system CCD camera.

2.12. Mammosphere formation assay

Breast cancer cells were collected, washed to remove sera, and then suspended in MammoCult™ Medium (StemCell Technologies). The cells were subsequently cultured at a density of 1000 cells/well for one to two weeks according to the manufacturer's instructions. Spheres were counted under a phase contrast microscope.

2.13. Chemotherapy drug treatment

Cancer stem cells (CSCs) and nonstem cancer cells (NSCCs) were sorted from MCF-7 cells treated with M1-S by flow cytometry using ALDEFLUORTM kit. The CSCs and NSCCs were treated with paclitaxel, 5-fluorouracil (5-FU), and doxorubicin for 24 h and cell viability was assessed by the sulforhodamine B (SRB) assay. The uptaken SRB was dissolved in 10 mM Tris solution and quantified by measuring the absorbance at 570 nm. The experiment was repeated twice.

2.14. Animal study

Four to five-week-old female Balb/C nude mice were subcutaneously implanted with 17β-estradiol pellets (Innovative Research, Novi, MI, USA). 24 h after implantation of the pellets, 5×10^2, 5×10^3, 5×10^4, or 5×10^5 CSCs or NSCCs sorted from M1-S-induced MCF-7 cells were inoculated into the right mammary fat pad of the mice. The mice were examined visually and by palpation at the site of injection twice weekly and tumor volumes calculated by using the following equation: $(\text{length}/2) \times (\text{width})^2$. At the end of the experiments, primary tumors were dissected.

To investigate the effect of the proinflammatory signals of macrophages on tumorigenesis of MDA-MB-231 cells, female Balb/C nude mice were subcutaneously injected with 5×10^3, 5×10^4, 5×10^5, or 5×10^6 MDA-MB-231 cells treated with or without THP-1-S or M1-S. The mice were examined visually and by palpation at the site of injection weekly. The tumors were dissected after sacrificing the animals. The lysates of the dissected tumors were prepared and subjected to SDS-PAGE and Western blot using the antibodies against ZEB1, fibronectin, Lin-28B, HMGA2, p-Stat3, p-p65, and GAPDH.

To analyze the direct role of the M1 macrophages in tumor formation, the 4–5-week old mice were subcutaneously co-injected with MDA-MB-231 cells and PBMC-derived proinflammatory macrophages. The tumors were measured with calipers weekly. The mice were sacrificed after 8 weeks and the tumors were dissected, fixed in formalin, and paraffin-embedded for immunohistochemical staining.

2.15. Statistical analysis

Statistical analyses were performed with SAS statistical software for Windows, Version 9.2 (SAS Institute). All data were presented as mean ± SD. Student's *t*-test or ANOVA was used for comparison between two groups. $P < 0.05$ was considered statistically significant. *

P < 0.05, ** P < 0.01.

3. Results

3.1. M1 macrophage induces CSC subpopulation in breast cancer cells

Human monocytic cell line THP-1 is widely used as a model for monocyte/macrophage differentiation. We produced polarized M1 and M2 macrophage from THP-1 and human monocytes according to established methods [28] (Supplemental Fig. 1A), which have also been used in studying the effect of polarized M1 on tumor cells both in vivo and in vitro [10,11]. THP-1 cells treated with IFN-γ/LPS firmly attached to the plates and most of the cells extended multiple elongated processes. IL-4/IL-13-induced cells were near-round and some cells had short broad cellular processes (Supplemental Fig. 1B). Stimulation by IFN-γ/LPS greatly increased the expression of CD197, a M1 macrophage marker, while the expression of M2 macrophage markers CD163 and CD206 was induced by IL-4/IL-13 (Supplemental Fig. 1C). To further characterize the macrophages, we analyzed the expression of cytokine genes associated with M1 or M2 phenotype. As shown in Supplemental Fig. 1D, the treatment with IFN-γ/LPS resulted in high production of IL-12, TNF-α, IL-1β, and IL-6, representing a typical proinflammatory phenotype. Following exposure to M2 polarizing mediators, cells produced elevated level of IL-10 and reduced level of IL-1β, IL-12, TNF-α, and IL-6. These data demonstrate that macrophages were functionally polarized by distinct stimuli, respectively.

Next, we cocultured human breast cancer cell line MCF-7, which belongs to luminal A-type cell line and displays non-advanced stage of breast cancer malignancy, with polarized M1 macrophages by utilizing a non-contact culture system and analyzed $CD24^{-/low}/CD44^{high}$ phenotype [29], which is one of the most consistently used biomarkers to identify breast CSCs. Fig. 1A and B show that after 6 hrs of M1 coculture, a subpopulation (9.9%) of $CD24^{-/low}/CD44^{high}$ was observed. The percentage of the subpopulation was further increased within 24 hrs (~23.2%), but remained steady after 48 hrs (22.7%). In MCF-7 control or MCF-7 cocultured with THP-1 cells, the subpopulation was at a very low level (1.9–2.0%). To confirm it, the expression of aldehyde dehydrogenase 1 (ALDH1), another functional marker of breast CSCs [30], was analyzed by Aldefluor flow cytometry-based assay. Similarly, the subpopulation of $ALDH1^+$ cells was induced (6.6%) at 6 h after coculture and reached to 13.8% at 24 h. The $ALDH1^+$ subpopulation was only about 1.2%–1.4% in the control groups. Similar results were observed in other M1-cocultured breast cancer cell lines, MDA-MB-231 (triple-negative breast cancer cell line) and T47D (luminal A-type cell line) cells (Supplemental Figs. 1E–1F). Moreover, we produced M1 macrophages from human peripheral blood mononuclear cells (PBMC) as previously described (Supplemental Fig. 1G). As is shown in Fig. 1C, coculture of MCF-7 cells with PBMC-derived M1 also generated a subpopulation of $ALDH1^+$ cells.

To better understand the correlations between M1 macrophages and CSCs in vivo, we analyzed their localization in tumor tissues of breast cancer patients. The paraffin-embedded breast cancer tissue sections of patients were co-labeled with antibodies against ALDH1 to identify CSCs and nitrogen-oxidase synthase 2 (NOS2) to detect M1 macrophages as previously reported [4]. As shown in Fig. 1D, a small number of $ALDH1^+$ cells were accumulated at the sites where $NOS2^+$ proinflammatory macrophages were also observed. This distribution of $ALDH1^+$ tumor cells in the close vicinity of macrophages displaying proinflammatory phenotype in breast cancer tissues implicates a potential functional link between M1 macrophages and CSCs.

To mimic what we observed in the samples of breast cancer patients, we co-inoculated a small amount of PBMC-polarized M1 macrophages (5×10^4) and a larger number of MDA-231 cells (1×10^6) into nude mice and measured tumor size every week (Supplemental Fig. 1H). Other groups have reported that injecting a much larger amount of polarized M1 macrophages (5×10^5–1×10^6) reduced established xenografts in mice models. Macrophages could have plastic phenotypes in response to different microenvironment signals, and thus the inoculated M1 macrophages might repolarize and could not be maintained in the original large number. In our assay, low amount of M1 macrophages enhanced tumorigenesis with a dramatic increase of tumor volume, implying that small number of M1 promoted tumor outgrowth by CSCs. Our data suggest that, when M1 macrophage is introduced to combat tumor bulk, maintaining a proper amount of M1 macrophages and inhibiting potential M1-induced CSC generation are both of great importance in the therapy.

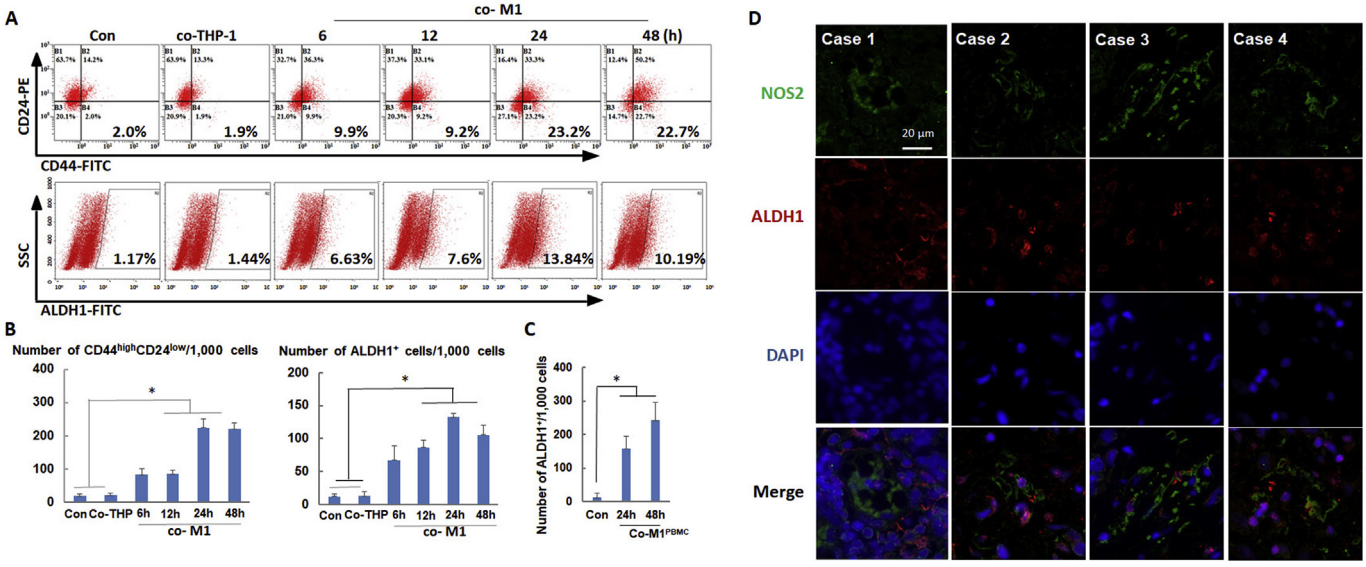

Fig. 1. M1 macrophages induce CSC phenotype in breast cancer cells A and B, MCF-7 cells were cocultured with THP-1-derived M1 macrophages (M1) for indicated time points. MCF-7 cells cocultured with or without untreated THP-1 cells were used as controls. $CD24^{low}/CD44^{high}$ phenotype was analyzed by flow cytometry. $ALDH1^+$ subpopulation was determined by Aldefluor flow cytometry-based assay. C, MCF-7 cells were cocultured with PBMC-derived M1 macrophages and $ALDH1^+$ subpopulation was analyzed. D, The paraffin-embedded breast cancer tissue sections were stained with antibodies against NOS2 and ALDH1 followed by fluorescein-labeled secondary antibodies incubation. Bar = 20 μm (con, control; co-M1/co-THP-1/co-$M1^{PBMC}$, cocultured with M1 macrophages/THP-1 cells/PBMC-derived M1macrophages).

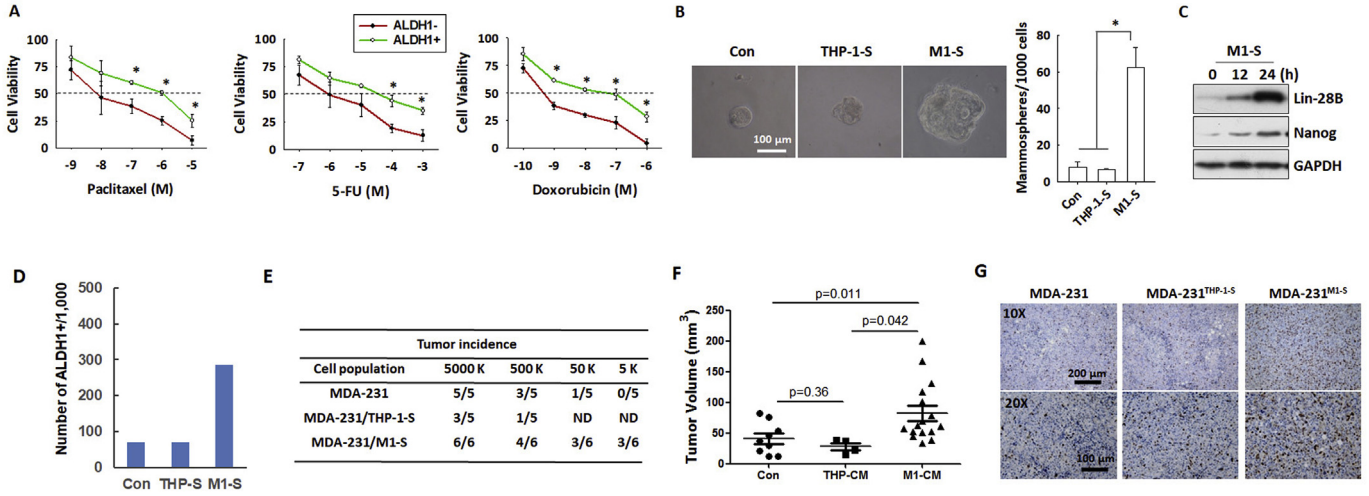

Fig. 2. M1 macrophages induce CSC phenotype A, After MCF-7 cells were treated with M1-S, ALDH1$^+$ and ALDH1$^-$ cells were sorted by flow cytometry using ALDEFLUOR™. The effects of chemotherapy drugs (paclitaxel, 5-FU, and doxorubicin) on the viability of CSCs and NSCCs were analyzed by SRB assays. B, MCF-7 cells were incubated with M1-S or the supernatant of THP-1 cells (THP-1-S). The cells were washed to remove serum, resuspended in MammoCult™ Medium, and subsequently cultured at a density of 1000 cells/well for one to two weeks. Spheres were observed and counted under an inverted microscope. Bar = 100 μm C, The expression of Lin-28B and Nanog was analyzed by Western blot. Images are shown for indicated proteins. D, MDA-MB-231 cells were treated with THP-1-S or M1-S for 24 h and ALDH1$^+$ cell frequency was analyzed by flow. E-G, 5×10^3, 5×10^4, 5×10^5 or 5×10^6 MDA-MB-231 cells treated with THP-1-S or M1-S were inoculated subcutaneously into mice. Tumor incidence (E) and tumor size (F) were evaluated. The expression of Ki67 in the tumor xenografts was detected by the rabbit polyclonal antibodies against Ki67 (G). Bar = 200 μm (THP-1-S/M1-S, the supernatant of THP-1 cells/proinflammatory) macrphages

3.2. M1 macrophages regulate CSC phenotype in a paracrine manner

To investigate how M1 macrophages regulate CSC phenotype in breast cancer cells, we incubated MCF-7 cells with the supernatant of M1 macrophages (M1-S). CD24$^{-/low}$/CD44^{high} cells were expanded in a time-dependent manner within 24 hrs (0 h, 2.7%; 12 h, 12.8%; 24 h, 19.8%; Supplemental Fig. 2A). This pro-CSC effect was verified by detecting ALDH1$^+$ subpopulation (0 h, 0.9%; 12 h, 8.9%; 24 h, 9.6%; Supplemental Fig. 2B).

Chemo-resistance is closely related to the intrinsic or acquired properties of CSCs [31]. To test whether M1-S-induced ALDH1$^+$ cells possess CSC properties, we sorted ALDH1$^+$ and ALDH1$^-$ cells from M1-S-treated MCF-7 cells and analyzed their viability after chemotherapy drugs (paclitaxel, 5-FU, and doxorubicin) treatment by SRB analysis. Fig. 2A shows that the ALDH1$^+$ cells were significantly more resistant to the chemotherapeutic agents than the ALDH1$^-$ subpopulation.

Another important property of CSC is to initiate tumor development in mice models at a low cell number. We introduced different numbers of ALDH$^+$ or ALDH1$^-$ cells from M1-S-treated MCF-7 cells into the fat pad of nude mice and found that injection of 500 ALDH1$^+$ cells could produce tumors in all the 3 mice, while no tumor was observed when 5×10^5 sorted ALDH1$^-$ cells were inoculated (Supplemental Fig. 2C). We further evaluated the stemness of M1-S-induced ALDH1$^+$ cells by testing tumor outgrowth in secondary mice. Since no tumor was formed by ALDH1$^-$ cells in mice and it was difficult to sort enough ALDH1$^+$ cells from MCF-7 cells which has been identified as luminal cells showing little to no ALDH activity, we used tumors (1×10^7 cell per mouse) formed by parental MCF-7 cells as control in the secondary implantation assay. The M1-S-induced ALDH1$^+$ tumor blocks exhibited rapid tumor re-growth in secondary recipient mice. However, the tumor blocks obtained from parental MCF-7 xenografts failed to produce palpable xenografts in recipient mice within 2 weeks after implantation (Supplemental Fig. 2D).

Mammosphere-formation assay was performed to analyze the self-renewal capacity of M1-S-treated MCF-7 cells. Fig. 2B shows that both the number and diameter of the spheres from M1-S-treated MCF-7 cells were much larger than those treated with or without THP-1 supernatant (THP-1-S). Western blot revealed that the pluripotent factors Lin-28B and Nanog were significantly upregulated in a time-dependent manner upon M1-S treatment (Fig. 2C).

To explore whether the pro-CSC effect of M1 macrophages is limited to certain breast cancer cell type, we used MDA-MB-231 cells, which display a more malignant phenotype, to see if the proinflammatory signal could also increase their tumorigenesis capacity. In order to have an overview of the effect of M1-S on MDA-231 cells before inoculating the cells into mice models, MDA-231 cells were treated with M1-S and the number of ALDH1$^+$ cells were identified to be increased (Fig. 2D). Next, different numbers of M1-S-treated MDA-MB-231 cells were injected into mice. Fig. 2E demonstrates that M1-S-treated MDA-MB-231 cells obtained a higher tumorigenic capability, as 5×10^3 cells could produce tumors, while no tumors were established when the same number of parental MDA-MB-231 cells were injected. Moreover, xenografts formed by M1-S-treated MDA-MB-231 cells grew more rapidly than untreated and THP-1-S-treated cells, as demonstrated by tumor volume and Ki67 staining (Fig. 2F and G). These data indicated that M1 might promote tumor growth through CSCs in a paracrine manner.

3.3. M1 macrophages induce EMT in breast cancer cells

It has been proposed that EMT is a major mechanism responsible for CSCs formation and that TAMs contribute to tumor progression by inducing EMT [32–34]. We found that compared to control groups, M1-S induced an obvious mesenchymal morphological alteration in MCF-7 cells, changing from a tightly packed epithelial-like morphology to an elongated spindle-like one (Fig. 3A). The expression level of epithelial marker E-cadherin was greatly reduced, while the mesenchymal marker fibronectin and E-cadherin transcription repressor ZEB1 were dramatically increased. Additionally, Lin-28B and HMGA2, which have been identified to be the key regulators in Oncostatin M (OSM)-induced EMT in our previous study and are suggested to be associated with CSC stemness by other groups, were also significantly upregulated in a time-dependent way within 24 h (Fig. 3B and C). The reduction of E-cadherin at cytoplasmic membrane and elevation of perinuclear aggregation of fibronectin in MCF-7 cells after M1-S treatment was further demonstrated by immunofluorescence (Fig. 3D). The phenotypic transition was also observed in MCF-7 cells cocultured with M1 macrophages either derived from THP-1 cells or PBMC (Fig. 3E and F). Notably, Stat3

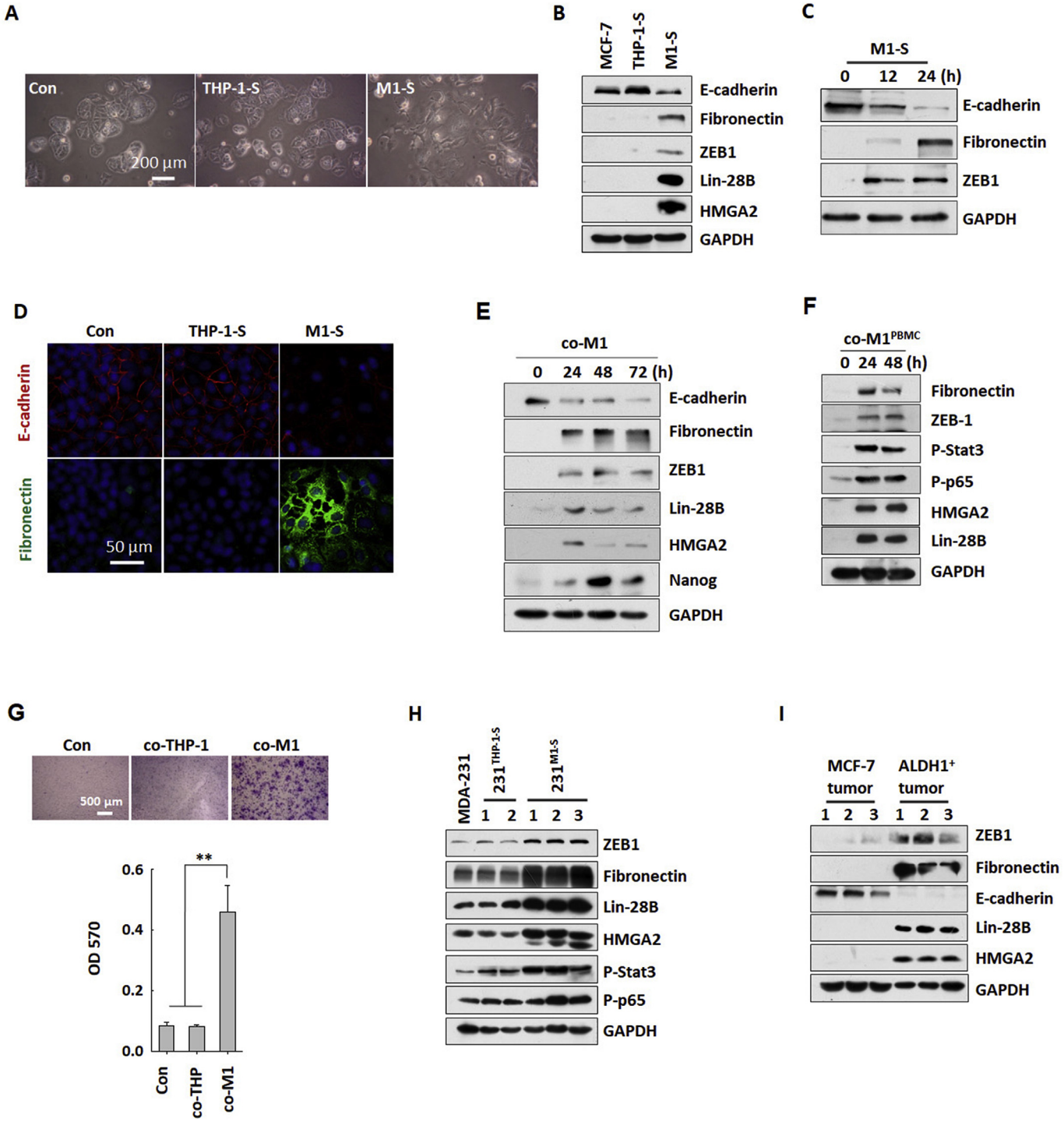

Fig. 3. M1 macrophages induce EMT in breast cancer cells A, MCF-7 cells were treated with THP-1-S or M1-S for 24 hrs and observed under an inverted microscope. Bar = 200 μm B, MCF-7 cells were treated with THP-1-S or M1-S. The expression of E-cadherin, fibronectin, ZEB-1, Lin-28B, and HMGA2 was analyzed by Western blot. Images are shown for indicated proteins. C, MCF-7 cells were treated with M1-S for indicated time points. The expression of E-cadherin, fibronectin, and ZEB-1 was analyzed. D, MCF-7 cells treated with THP-1-S or M1-S for 24 h were subjected to immunofluorescence assay to detect the localization and expression of fibronectin and E-cadherin. DAPI was used to stain nuclear. Images were obtained under a laser scanning confocal microscope. Bar = 50 μm E and F, MCF-7 cells were cocultured with M1 macrophages polarized from THP-1 cells (E) or PBMC (F). The expression of EMT/CSC-associated molecules was analyzed. G, MCF-7 cells were co-cultured with THP-1 cells or THP-1-derived M1 macrophages. The invasive activities of the cells were analyzed by Matrigel invasion assay. Bar = 500 μm H, The tumor tissues were dissected from tumors formed by THP-1-S-treated or M1-S-treated MDA-MB-231 cells. The expression of EMT/CSC-associated molecules was analyzed. Images are shown for indicated proteins. I, Tumor tissues were dissected from the parental MCF-7 cells-formed xenograft or tumors formed by M1-S-induced ALDH1$^+$ MCF-7 cells. The expression of EMT/CSC-associated molecules was analyzed.

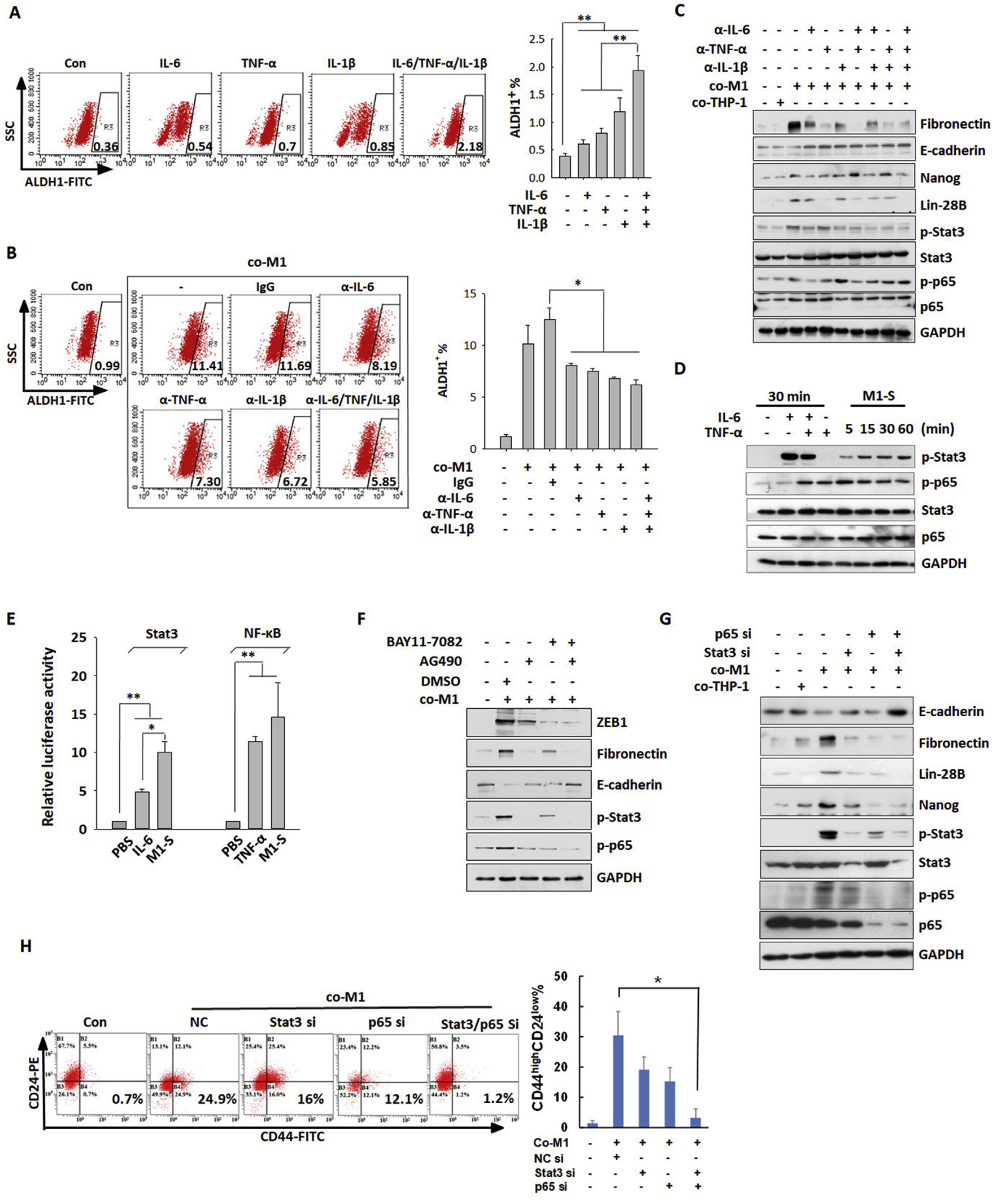

(caption on next page)

and NF-κB p65 subunit, which participate in a variety of processes that related to tumor malignancy, were markedly activated.

This EMT-like process was accompanied by an enhanced invasive potential of MCF-7 cells (Fig. 3G). Similar data were obtained in MDA-MB-231, T47D, and BT474 cells (Supplemental Figs. 3A–3E). Compared with xenografts formed by MDA-MB-231 treated with or without THP-1-S, tumors arising from M1-S-treated MDA-MB-231 cells displayed a more malignant phenotype with higher levels of ZEB1, fibronectin, Lin-

Fig. 4. Stat3 and NF-κB inflammatory pathways are involved in induction of EMT/CSC A, MCF-7 cells were treated with IL-6, TNF-α, and IL-1β and ALDH1$^+$ population was analyzed. B and C, MCF-7 cells were cocultured with M1 macrophages and neutralizing antibodies against IL-6, TNF-α, or IL-1β. ALDH1$^+$ cells were analyzed by flow cytometry (B). The expression of EMT/CSC-associated molecules and activation of Stat3 and NF-κB were analyzed by Western blot (C). D, MCF-7 cells were treated with M1-S. The treatment with IL-6 and TNF-α was used as controls. The phosphorylated Stat3 and p65 were analyzed. Images are shown for indicated proteins. E, MCF-7 cells were co-transfected with 300 ng of Stat3 or NF-κB luciferase reporter plasmid and 30 ng of pRL-TK reporter plasmid. After 24 h, the cells were treated with M1-S. The luciferase activities were measured using Dual-Luciferase Reporter Assay System and normalized to Renilla luciferase activities. F, MCF-7 cells were co-cultured with M1 macrophages with an addition of JAK2 inhibitor AG490 or NF-κB inhibitor BAY11-7082. The expression of EMT/CSC-associated molecules and activation of Stat3 and p65 were analyzed. Images are shown for indicated proteins. G and H, MCF-7 cells were transfected with 50 nM specific siRNAs targeting Stat3 or p65. The transfected cells were cocultured with THP-1-derived M1 macrophages or THP-1control cells for 24 h. The expression of EMT/CSC-associated molecules and activation of Stat3 and p65 were analyzed by Western blot (G). Images are shown for indicated proteins. The CD24$^{-/low}$/CD44^{high} population was analyzed by flow cytometry (H). (α-IL-6/α-TNF-α/α-IL-1β, the antibodies against IL-6/TNF-α/IL-1β).

28B, HMGA2 and phosphorylated Stat3 and p65 (Fig. 3H).

Similarly, xenografts formed by sorted M1-S-induced ALDH1$^+$ cells displayed a less epithelial phenotype than tumors generated by parental MCF-7 cells. Fig. 3I shows that in contrast to MCF-7 control tumors, M1-S-induced ALDH1$^+$ tumors express lower level of E-cadherin and higher level of mesenchymal marker fibronectin and EMT/CSC-associated molecules ZEB-1, Lin-28B, and HMGA2. These results suggest that EMT/CSC program could be activated by M1 macrophages in breast cancer cells.

3.4. Stat3 and NF-κB pathways are activated in M1-induced EMT/CSC

It has been known that inflammation acts as a crucial mediator of EMT [35]. M1 macrophages secrete high amounts of proinflammatory mediators, including TNF-α, IL-1β and IL-6. Our data showed that M1 macrophages induced CSCs in a paracrine way. Therefore, in order to investigate the effects of M1-characterised cytokines on CSC induction, we treated MCF-7 cells with IL-6, TNF-α, and IL-1β. The combinational stimulation resulted in an induction of ALDH1$^+$ subpopulation (Fig. 4A). To further confirm the role of these cytokines in CSC induction, we cocultured MCF-7 cells with M1 macrophages in the presence of neutralizing antibody against IL-6, TNF-α, or IL-1β and observed the antagonizing effect of these neutralizing antibodies on CSC induction (Fig. 4B). Meanwhile, the upregulation of fibronectin and Lin-28B was dramatically reversed and E-cadherin expression restored (Fig. 4C). We noticed that the induction of CSC subpopulation by addition of cytokines was not as strong as M1-S and the neutralization antibodies did not block CSC generation completely, which indicated that IL-6, TNF-α and IL-1β play a partial role in M1-induced CSC formation and other cytokines might also be involved. These data implicate a proinflammatory cytokine network functioning in M1-induced EMT/CSC process.

Many proinflammatory cytokines are reported to play their roles by converging on Stat3 and NF-κB pathways [36]. In M1-treated MCF-7 cells, Stat3 and NF-κB were activated (Fig. 4C). Fig. 4D demonstrated that, using IL-6 or TNF-α as positive control, M1-S led to a rapid activation of both Stat3 and p65. As determined by luciferase reporter gene assays, Stat3-and NF-κB-driven luciferase activities were increased by approximately 10 and 15 folds in the presence of M1-S, respectively. Particularly, the activity of Stat3-dependent luciferase reporter was much higher in the M1-S-treated cells than in the IL-6-treated cells (Fig. 4E). Recently, our group has reported that motivation of Stat3 could “switch on” EMT in breast cancer cells [26] and IL-6/Stat3 pathway was involved in transuzumab-resistance associated EMT/CSC in gastric cancer [27]. Here, we found that Janus kinase 2 (JAK2) inhibitor AG490 and NF-κB inhibitor BAY11-7082 greatly blocked the effects of M1 macrophages on EMT in the cocultured MCF-7 cells (Fig. 4F). Blocking both pathways more effectively reversed the malignancy phenotype. The roles of Stat3/NF-κB pathways in induction of EMT/CSC were confirmed by knockdown assays. The maximal effect on reversing EMT/CSC was caused by simultaneous repression of Stat3 and p65 (Fig. 4G). In Fig. 4G, when both Stat3 and p65 were knocked down in MCF-7 cells, reduction of E-cadherin by M1 was reversed, while M1-stimulated induction of Fibronectin and CSC-related genes (Lin-28B, Nanog) was inhibited. Meanwhile, CD24$^{-/low}$/CD44^{high} subpopulation and invasive activities induced by M1 macrophages were also reduced by siRNA-mediated Stat3 and p65 knockdown in MCF-7 cells (Fig. 4H and Supplemental Fig. 4A). Ectopic overexpression of p65 or Stat3C (a constitutive active form of Stat3) modestly upregulated Lin-28B and Nanog (Supplemental Fig. 4B). These data indicate that cytokine-induced activation of Stat3/NF-κB pathways is critical to M1-induced EMT/CSC process.

3.5. Lin-28B-let-7-HMGA2 axis regulates proinflammatory signals-initiated CSC formation

Our previous study has revealed a key role of Stat3-coordinated Lin-28B-let-7-HMGA2 axis in initiating OSM-induced EMT in breast cancer cells. Other groups also have reported the role of these molecules in tumor malignancy. Recently, Lin-28B/let-7/HMGA2 has been proved to function in regulating self-renewal potential of fetal hematopoietic stem cells [37]. We found that M1-S significantly upregulated Lin-28B/HMGA2 expression and downregulated the level of let-7 in MCF-7 cells (Fig. 5A). A much stronger activation of this axis was observed in co-culture system. As an initiator of this axis, Lin-28B plays a critical role in inducing phenotype transition. Knockdown of Lin-28B in MDA-MB-231 cells, which are highly invasive and display all the characteristics of post-EMT, downregulated fibronectin expression (Supplemental Fig. 5A). In contrast, overexpression of Lin-28B in MCF-7 cells, which exhibit the features of more differentiated luminal epithelial cells, remarkably repressed the expression of E-cadherin, yet induced the expression of fibronectin (Supplemental Fig. 5B). In a variety of human cancers, Lin-28B selectively blocks the expression of let-7 and HMGA2 is one of let-7 target genes. Transfection of specific siRNA targeting Lin-28B or HMGA2 markedly reduced the percentage of the ALDH1$^+$ subpopulation and the invasive activities of MCF-7 cells cocultured with M1 macrophages (Fig. 5B and C). Though the suppressive effect of let-7 mimics on ALDH1$^+$ subpopulation was not statistically significant, the transfection of let-7 mimics dramatically reduced M1-induced invasive capability of MCF-7 cells (Fig. 5C).

In our previous study, we have demonstrated that HMGA2 acts as a master switch of OSM-induced-EMT. To determine the role of HMGA2 in M1-induced-EMT/CSC, we established MDA-MB-231 cells that stably expressed HMGA2-shRNA plasmid (MDA-MB-231/HMGA2sh). The sphere formation capacities of MDA-MB-231/HMGA2sh cells were significantly decreased (Fig. 5D). Repression of HMGA2 expression not only increased E-cadherin expression directly but also reduced M1-S-induced upregulation of ZEB1 and fibronectin (Fig. 5E). In MCF-7 cells, the mRNA level of CSC-associated molecules Krüppel-like factor (KLF)-4 and Nanog that were increased by M1 was remarkably suppressed when HMGA2 siRNA were introduced (Fig. 5F). These data suggest that Lin-28B-let-7-HMGA2 axis is critical in M1-induced EMT/CSC and HMGA2 functions as the key regulator in this axis.

3.6. Macrophages regulate CSC generation and maintenance through phenotype transdifferentiation

We noticed that the percentage of the CD24$^{-/low}$/CD44^{high} or

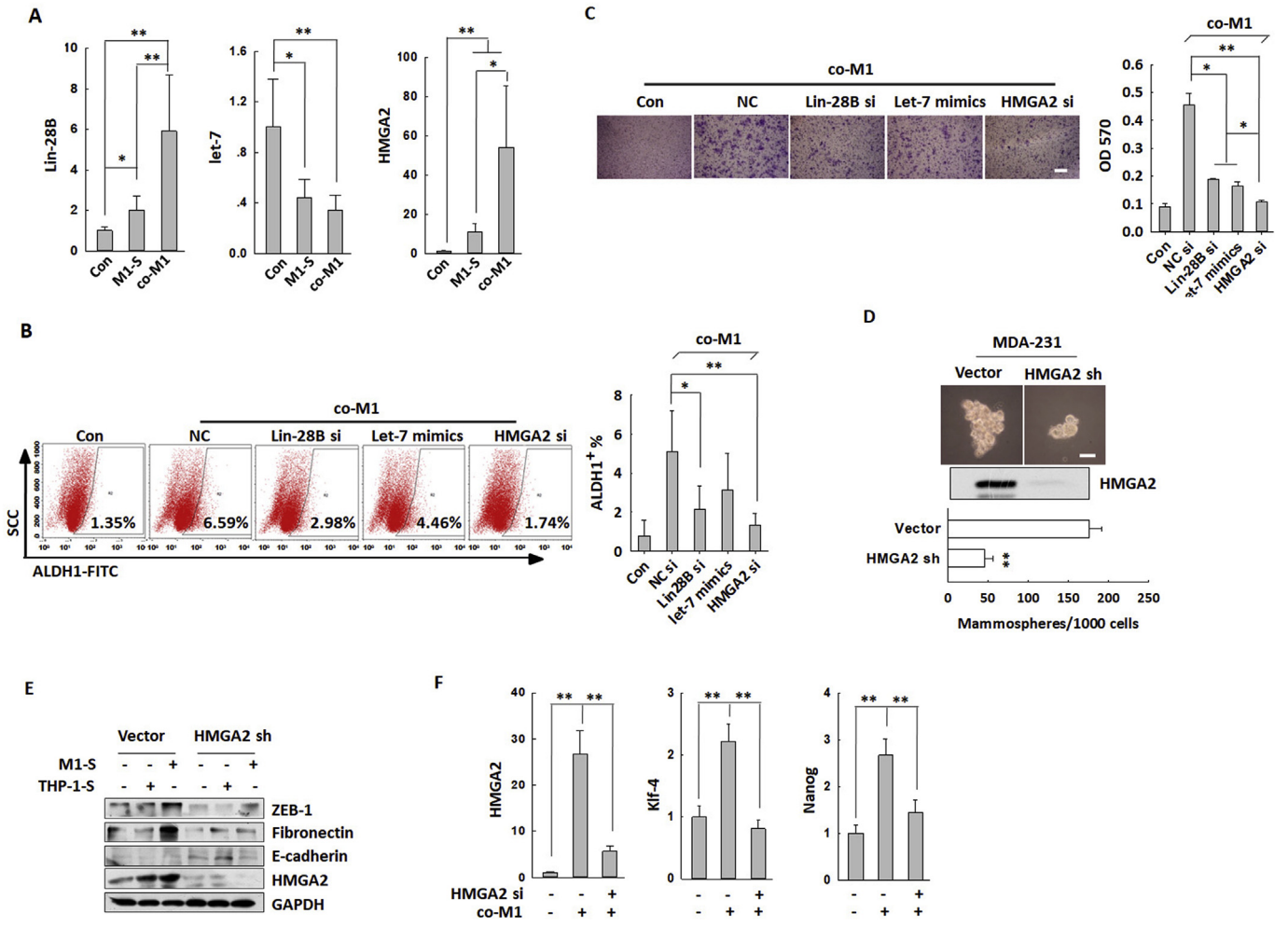

Fig. 5. Lin-28B-let-7-HMGA2 axis regulates M1-induced EMT and CSC formation A, MCF-7 cells were incubated with M1-S or cocultured with M1 macrophages for 24 h. The expression of Lin-28B, let-7, and HMGA2 at mRNA levels were determined by real-time PCR. B and C, MCF-7 cells were transfected with 50 nM specific siRNAs targeting Lin-28B and HMGA2 or with let-7 mimics. The transfected cells were cocultured with M1 macrophages. The ALDH1$^+$ cells were analyzed by flow cytometry (B) and the invasive activities of the cells by Matrigel invasion assays (C). D, MDA-MB-231 cells that were stably transfected with the plasmid expressing HMGA2-shRNA (MDA-MB-231/HMGA2sh) or empty plasmid were incubated with M1-S. The sphere formation capacities of the cells were evaluated. E, MDA-MB-231/HMGA2sh or control cells were treated with THP-1-S or M1-S. The expression of EMT/CSC-associated molecules was analyzed by Western blot. F, MCF-7 cells transfected with HMGA2 siRNA were cocultured with M1 macrophages. The mRNA level of HMGA2, Klf-4, and Nanog was analyzed by real-time PCR.

ALDH1$^+$ subpopulation in MCF-7 cells was progressively increased within the first 24 hrs of coculture with M1 macrophages (Fig. 1A). However, afterwards, the ratio did not further expand, suggesting a potential mechanism to maintain a relatively stable subpopulation of CSCs. Macrophages are functionally plastic and their phenotype characteristics associate with different stages of tumor development, with M1-like phenotype in the site of chronic inflammation where tumor develops and M2-like phonotype in established tumors [38]. In contrast to immunosuppressive micromilieu in tumor nest, the peritumoral stroma contains macrophages with proinflammatory phenotypes [39], implying different phenotype of macrophage may function in different tumor stage.

To investigate whether M1 and M2 macrophages exert differential effect on CSCs, MCF-7 cells were treated with M1-S and M2-S, respectively. Fig. 6A shows that a much higher proportion of CD24$^{-/low}$/CD44^{high} or ALDH1$^+$ subpopulation was observed in M1-S- than M2-S-treated cells. CSCs (ALDH1$^+$) and NSCCs (ALDH1$^-$) were sorted and cultured with THP-1-S, M1-S, and M2-S, respectively. When NSCCs were treated with M1-S for 24 h, a subpopulation of ALDH1$^+$ cells (10.2%) was observed, whereas the effects of the THP-1-S (2.28%) and M2-S (3.7%) on CSC induction were much weaker (Fig. 6B), supporting that CSCs can be directly induced from NSCCs by M1 macrophages. Following exposure of sorted CSCs to M1-S for 4 days, the proportion of ALDH1$^+$ cells reduced to 3.53%, whereas a higher percentage (8.34%) of the subpopulation was detected by M2-S, implying that M2-S contributes more to the maintenance of stemness. Both M1 and M2 macrophages upregulated the expression of CSC-associated molecules Lin-28B, Nanog, Klf-4, c-Myc, and Oct-4. However, the upregulation of Lin-28B, Klf-4, and Oct-4 was more pronounced in M1-cocultured group (Fig. 6C). Similar data were obtained by treating BT474 cells with the supernatants of macrophages (Supplemental Fig. 6A). Lin-28B, Nanog, Klf4, and Oct4 are known as core reprogramming factors in reprogramming somatic cells [40,41], implying that M1 are more potent in generating CSCs. Additionally, the activation of EMT (downregulation of E-cadherin and upregulation of Fibronectin and Lin-28B) and Stat3/NF-κB pathways by M1-S was more striking (Supplemental Fig. 6A), which may explain the stronger effect of M1 on CSC formation. The data suggest that macrophages may modulate CSC formation and maintenance by combining proinflammatory and immunosuppressive signals.

It has been revealed that blood circulating monocytes treated with tumor culture supernatants transiently acquired an activated proinflammatory phenotype before their subsequent re-polarization into immunosuppressive macrophages [39]. In our study, the surface

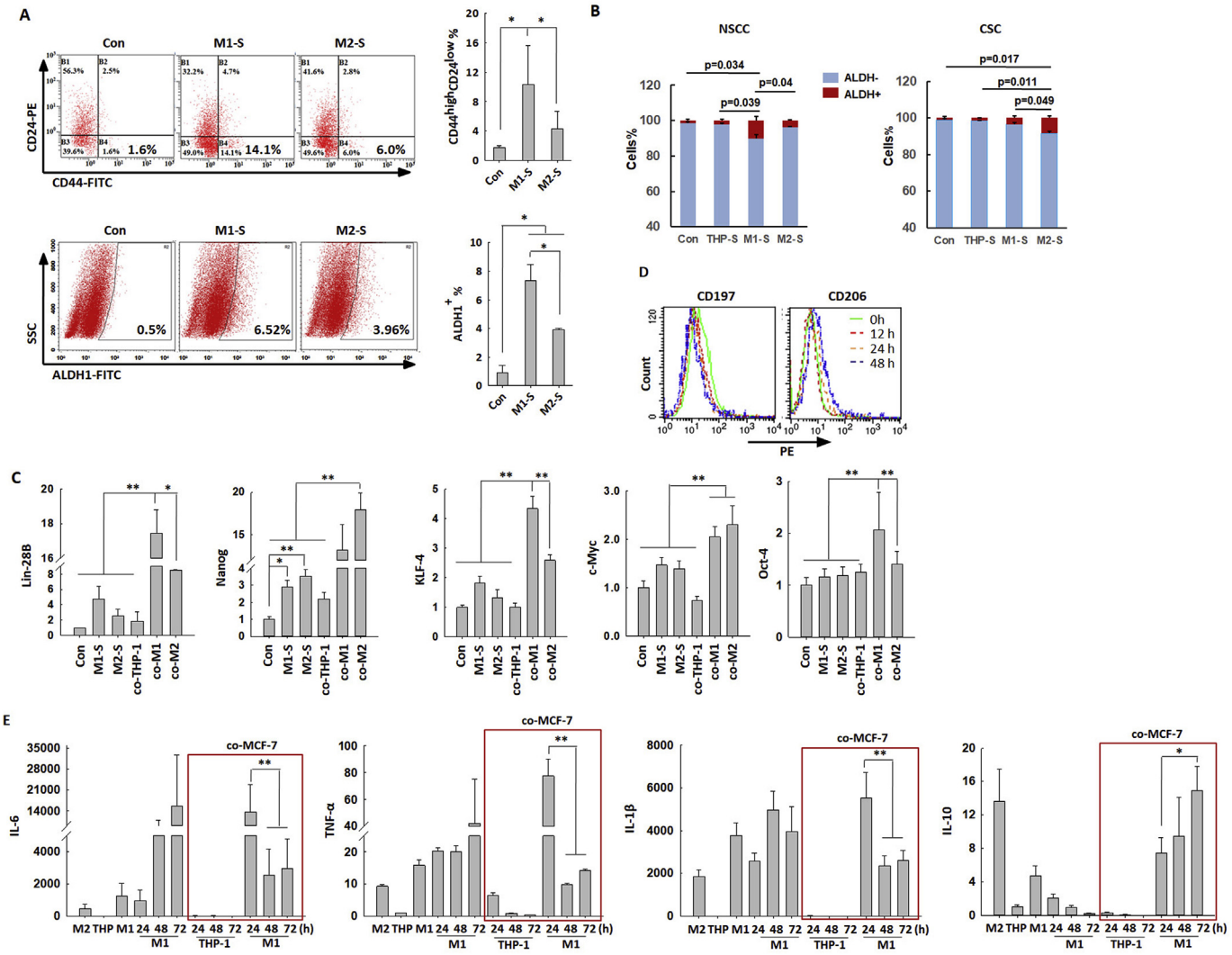

Fig. 6. Macrophages regulate CSC generation and maintenance through proinflammatory and immunosuppressive signals shifting A, MCF-7 cells were incubated with M1-S or M2-S. $CD24^{-/low}/CD44^{high}$ and $ALDH1^{+}$ subpopulations were analyzed by flow cytometry, respectively. B, $ALDH1^{+}$ and $ALDH1^{-}$ were sorted by flow cytometry and then treated with THP-1-S, M1-S, or M2-S, respectively. The percentage of $ALDH1^{+}$ population was analyzed. C, MCF-7 cells were treated with M1-S, or M2-S, or cocultured with THP-1 cells, M1 or M2 macrophages for 24 h. The expression of Lin-28B, Nanog, Klf-4, c-Myc, and Oct-4 was analyzed. D and E, M1 macrophages were cocultured with MCF-7 cells for 24, 48, and 72 h. The phenotypes of the macrophages were analyzed by flow cytometry at indicated time points (D). The expression of IL-6, TNF-α, IL-1β, and IL-10 at mRNA level was determined by real-time PCR (E).

markers of M1 or M2 macrophages were not significantly shifted within the first 24 h of coculture with MCF-7 cells (Supplemental Fig. 6B). Intriguingly, IL-6, IL-1β, TNF-α, and IL-10 were significantly upregulated in both cocultured M1and M2 macrophages during this period (Supplemental Fig. 6C). Our previous data showed that the CSC subpopulation was observed as early as 6 h after coculture with M1 macrophages, which excludes the possibility that generation of CSCs was induced by M2 macrophages repolarized from M1. Of note, cocultured M2 macrophages displayed a combined proinflammatory/immunosuppressive phenotype with increased levels of IL-1β, TNF-α and IL-12 (Supplemental Fig. 6C). These data suggested that the proinflammatory signals of macrophages might be required for CSC formation.

We further analyze the dynamic alterations of cocultured macrophages over time. After 48 h of coculture with MCF-7 cells, a slight increase of CD206 expression as well as a trivial decrease of CD197 was observed in cocultured M1 macrophages (Fig. 6D). Cytokine profile revealed that the proinflammatory phenotype was enhanced within 24 h. However afterwards, the levels of IL-6, TNF-α, and IL-1β were remarkably declined and the expression of IL-10 was progressively elevated (Fig. 6E), indicating macrophage repolarization was undergoing. Consistently, the timing of the transient enhancement of activation (~24 h) and the subsequent acquisition of M2 phenotype (~48 h) are consistent with the timing of the induction and maintenance of CSCs. Therefore, the stagnant of CSC generation after 24 h may be attributed to the functional phenotype alteration of the macrophages. Taken together, M1 signals predominantly act in CSC formation, and macrophages regulate the initiation and maintenance of CSCs by orchestrating proinflammatory and immunosuppressive signals (Supplemental Fig. 7).

4. Discussion

Nowadays, it has been widely accepted that tumorigenesis is orchestrated by innate immunity [42]. As a major component in innate immunity and the most abundant immune cells infiltrating in solid tumor, macrophages regulate tumor initiation and progression. The phenotype of macrophage is considered to switch from proinflammatory M1 in tumorigenesis to immunosuppressive M2 since tumors are established, with its role changing from tumoricidal to pro-

malignant in tumor. An increased M1/M2 ratio within tumors often suggests a better prognosis in various cancer patients. Moreover, immunosuppressive tumor microenvironment attenuates the efficacy of immunotherapy. TAMs have been demonstrated to express high level of PD-1, which impairs phagocytosis of activated macrophages and inhibits the effects of stimulated T cells. Additionally, PD-1$^-$ TAMs have been revealed recently to be capable of capturing anti-PD-1 antibody from PD-1$^+$ tumor-infiltrating CD8$^+$ T cells, thus impairing the tumoricidal effect of CD8$^+$ T cell [14]. Therefore, many attempts have been made to increase M1/M2 ratio in tumor microenvironment. 5,6-Dymethylxanthenone-acetic-acid was used to change the intratumoral M2/non-M2 immunosuppressive ratio by increasing the influx of neutrophils and M1 macrophages to the tumor, resulting in an increased number and activity of intratumoral CD8$^+$ T cells and enhanced efficacy of other immunotherapies [13]. Similarly, injection of a certain amount of THP-1-polarized M1 macrophages into established hepatocellular tumors in mouse models significantly reduced tumor volume. However, the induction of acute inflammatory response and the difficulty to retain injected immune cells in tumor sites hindered direct use of M1 macrophages in cancer treatment. To improve the strategy, a biocompatible scaffold composed of poly and gelatin-based hydrogel was created to support the function of M1 macrophages in targeting tumor cells in vitro and in vivo without affecting normal cells [11]. Though the killing capacity of M1 macrophages is promising in cancer treatment, the role of M1 macrophages in tumor has not received enough attention.

Actually, both M1 and M2 macrophages have been detected in various types of tumor tissues [4,15]. Though macrophages with proinflammatory phenotype in peritumoral stroma have been revealed to be educated towards M2 phenotype after infiltrating into tumor, these activated macrophages could trigger the proliferation of IL-17-producing CD8$^+$ T cells whose infiltration promoted hepatocellular carcinoma progression and positively related to poor survival of cancer patients [43] and the transient state of activation is also critical for M2 re-polarization. The findings in *H. pylori*-associated gastric cancer suggest that the proinflammatory macrophage polarization during *H. pylori* infection contributes to gastric carcinogenesis as a result of increased levels of reactive oxygen and nitrogen species [44]. Very recently, it has been revealed that treatment with polarized M1 macrophages enhances the metastasis potential of ovarian cancer cell lines via NF-κB pathway [19]. M1 TAMs isolated from PDAC patients, as well as in vitro generated M1 macrophages, mediated EMT in premalignant and malignant pancreatic ductal epithelial cells [15]. Therefore, it is worth studying whether the proinflammatory signals of M1 macrophage have side effects when combating tumor cells. In our study, we used both culture media of macrophages and co-culture system to treat breast cancer cells and found that besides killing breast cancer cells, the proinflammatory signals of M1 macrophages functioned as a driving force for CSC generation. Stat3/NF-κB pathways were activated by a proinflammatory cytokine network (IL-6, TNF-α, IL-1β included), leading to Lin-28B-let-7-HMGA2 axis-induced EMT/CSC in breast cancer cells. Also, we found that a small number of NOS2$^+$ M1 macrophages were observed within the samples of breast cancer patients and frequently present in close proximity to ALDH1$^+$ CSCs. Our findings are in line with the report showing that although being localized in close proximity to cancer cells, macrophages were hardly detected in direct cell-cell contact with tumor cells [16], supporting the view that macrophages contribute to malignancy in a paracrine manner. Instead of inoculating a higher percentage of polarized M1 macrophages, we co-injected a smaller amount of PBMC-polarized M1 macrophages (5×10^4) with MDA-MB-231 cells in mouse model and achieved an increase in the size of xenografts. Moreover, a higher tumor incidence was achieved with M1-S-treated MDA-MB-231 cells, and as few as 5×10^3 cells led to tumor growth in mice. Actually, some investigations have shown a mixed proinflammatory/immunosuppressive phenotype in tumor-associated macrophages [38,45,46]. On the other hand, exosomes secreted by melanoma endowed macrophages a mixed M1/M2 phenotype to promote tumor malignancy [47]. In our study, we also found an increased level of IL-6, TNF-α and IL-1β in polarized M2 macrophages cocultured with breast cancer cells, suggesting that "proper" amount of proinflammatory signals function in tumor progression and the phenotype of tumor-associated macrophages is more complicated. Whatever, since M1 is the prevailing phenotype of macrophages in chronic inflammation when tumor develops, our data indicated that M1 signals contribute to tumor development by initiating CSC formation.

CSCs have been implicated as a major cause for recurrence, metastasis, and therapeutic resistance, leading to therapy failure and mortality in cancer patients. However, the mechanisms of CSC generation still remain unclear. It is of great importance to explore how and when CSC is generated and thus to reduce the possibility of CSC formation and to target CSCs by blocking critical molecules and pathways in cancer therapy.

Many of the signaling pathways associated with induction of EMT are suggested to be involved in development and maintenance of CSCs. The key regulators of EMT, including ZEB1, Snail/Slug, and Twist, also modulate the stemness of somatic stem cells and CSCs [48–50]. Previously, we reported that the activation of IL-6/Stat3 pathway induced EMT and CSC phenotype in gastric cancer cells through a positive feedback loop with Jagged-1/Notch pathway. Moreover, in chronic psychological stress in breast cancer, we have found that monocytes/macrophages contribute to the pre-metastasis niche of lung. Tumor-associated monocytes and macrophages have been reported to create a niche to enhance CSC activities through juxtacrine signaling with CSCs. CD90 and EphA4 could be upregulated after EMT on carcinoma cells to mediate the physical interactions of CSCs with TAMs, which activates NF-κB in CSCs to sustain the stem cell state by inducing the secretion of a variety of cytokines [34]. Our previous study demonstrated that macrophage-derived OSM initiated EMT process in breast cancer cells by activating the Stat3-regulated Lin-28B-let-7-HMGA2 axis [26]. Intriguingly, molecules in this axis participate in regulating stemness markers (Oct-4, Sox-2, Nanog) and inducing reprogramming and transdifferentiation of somatic cells. Lin-28B positively regulates the expression of Oct-4 and Sox2 and self-renewal of embryonic stem cells [51,52]. Let-7 miRNA biogenesis is blocked by Lin-28B, resulting in repression of the let-7 target genes [53]. It has been proposed that let-7 regulates stemness by repressing self-renewal and promoting differentiation in both normal development and CSCs [54]. HMGA2, as a target of let-7, was a specific modulator of neural and embryonic stem cell self-renewal potential [55,56]. Like Lin28B, HMGA2 regulates Sox-2 expression by directly binding to its promoter [57]. A recent study indicates that Lin-28B-let-7-HMGA2 axis controls high self-renewal potential of fetal hematopoietic stem cells [37]. In the current study, we demonstrate that the proinflammatory signals of M1 macrophages induce stemness properties in non-stem breast cancer cells through Stat3/NF-κB-induced Lin-28B-let-7-HMGA2 activation. Notably, HMGA2 functions as a determinant factor in this axis. Suppression of HMGA2 expression directly reversed the proinflammatory signals-induced expression of reprogramming factors Klf-4 and Nanog, repressed mammosphere formation, and reduced ALDH1$^+$ subpopulation. Our data suggest that as a critical regulatory axis for in CSC occurrence, Lin-28B-let-7-HMGA2 is a potential target in cancer treatment.

We also noticed that after 24 hrs of coculture with proinflammatory macrophages, the CSC population in breast cancer cells was no longer increased. It is known that the phenotype of tissue macrophages is not an immutable end-stage phenotype. Once infiltrating into tumor nest, the activated macrophages tend to be re-polarized into M2 phenotype in response to microenvironmental signals. We found that within the first 24 hrs of coculture when CSC population reached to its peak, M1 macrophage predominantly possessed proinflammatory phenotype. However, the level of IL-12 was decreased, while IL-10 increased, indicating macrophage re-polarization was undergoing. After coculture for 48 hrs, the functional phenotype of the macrophages was similar to

that of M2 macrophages given the expression level of IL-6, IL-1β, TNF-α, and IL-10. Concomitantly, the proportion of CSCs remained relatively steady. Furthermore, M1-S directly induced ALDH1^{+} subpopulation from sorted ALDH1^{-} cells and was more potent in upregulating the expression of the core reprogramming factors Lin-28B, Klf-4 and Oct-4, while M2-S was more efficient in maintaining the CSC phenotype, which implicates that macrophages play a potential role in inducing and maintaining CSCs through orchestrating proinflammatory and immunosuppressive signals.

Diversity and plasticity are hallmarks of macrophages. Classical M1 and alternative M2 activation of macrophages, possessing opposite functions, represent two extremes of a dynamic changing state of macrophage polarization in response to different microenvironment stimulus. Tumor microenvironment, including macrophages, could be targeted for effective therapy to combat cancers. Two attractive therapeutic strategies are being investigated: targeting M2 TAMs and reprogramming TAM to antitumor phenotype. It has been reported that TAM-specific molecules, including mannose receptor CD206, stress protein Legumain, and scavenger receptor A and CD52, could serve as efficient targets for cancer treatment [58–60]. IRF/STAT signaling is a central pathway in regulating M1-M2 polarization. Activation of IRF/STAT1 by IFNs and TLR would skew macrophage function towards M1 phenotype, while activation of IRF/STAT6 signaling by IL-4 and IL-13 would polarize macrophages towards M2 phenotype [61]. Activation of NF-κB is critical in polarization of TAM to antitumor phenotype via TLR agonists, anti-CD40 mAbs, and IL-10 mAbs [62]. Pseudomonas aeruginosa mannose-sensitive hemagglutinin could re-educate CD163 $^{+}$ TAM to M1 phenotype in malignant pleural effusion [63]. Recently, it has been suggested that bioconjugated manganese dioxide nanoparticles enhanced the responses of chemotherapy by inducing M2 TAMs towards M1 phenotype [64]. The use of β-glucan is also currently under investigation for their antitumor properties by differentiating M2 macrophages into M1 [65].

Taken together, our data indicate that the proinflammatory signals of M1 macrophage may be one of the driving forces in the development and expansion of CSC at the early stage of tumorigenesis. Lin-28B-let-7-HMGA2 axis plays a critical role in CSC formation. The functional phenotypic transition of macrophages imposed by interplay with tumor microenvironment dictates the fate of CSCs. Therefore, it is not safe to determine M1 as absolutely “good” and cancer progression may need both M1 and M2 signals [66,67]. M1 macrophages are now being reported to be powerful in killing cancer cells and being tested in cancer treatment, so it is of great importance to inhibit M1 signal-induced CSC generation and repress M2 repolarization by targeting critical pathways and molecules.

Compliance with ethics guide lines

All authors declare they have no conflict of interest. This study was approved by the ethics committee of Institute of Basic Medical Sciences. All animal studies were performed in accordance with the institutional guidelines and the experiments were approved by the Animal Care and Use Committee of the institute.

Conflicts of interest

All authors read and approved the final version of the manuscript, and the authors declare no conflict interest.

Acknowledgements

Grant Support: National Key Technologies R&D Program for New Drugs (2013ZX09102056), the National High-Tech Research and Development Plan (863 Program, No. 2014AA020604), National Natural Science Foundation of China (No. 31500702, 31370825, 81272232, 81402562, 81572845, and 81401311), Beijing Natural Science Foundation (No. 7162144, 7122124, and 7132163), and China Postdoctoral Science Foundation (No. 2015T81095). The authors are grateful to all staffs who contributed to this study.

Appendix A. Supplementary data

Supplementary data to this article can be found online at https://doi.org/10.1016/j.canlet.2019.03.032.

References

[1] D.I. Gabrilovich, S. Ostrand-Rosenberg, V. Bronte, Coordinated regulation of myeloid cells by tumours, Nat. Rev. Immunol. 12 (2012) 253–268.
[2] S. Sousa, R. Brion, M. Lintunen, P. Kronqvist, J. Sandholm, J. Monkkonen, P.L. Kellokumpu-Lehtinen, S. Lauttia, O. Tynninen, H. Joensuu, D. Heymann, J.A. Maatta, Human breast cancer cells educate macrophages toward the M2 activation status, Breast Cancer Res. 17 (2015) 101.
[3] M. Zhang, Y. He, X. Sun, Q. Li, W. Wang, A. Zhao, W. Di, A high M1/M2 ratio of tumor-associated macrophages is associated with extended survival in ovarian cancer patients, J. Ovarian Res. 7 (2014) 19.
[4] S. Edin, M.L. Wikberg, A.M. Dahlin, J. Rutegard, A. Oberg, P.A. Oldenborg, R. Palmqvist, The distribution of macrophages with a M1 or M2 phenotype in relation to prognosis and the molecular characteristics of colorectal cancer, PLoS One 7 (2012) e47045.
[5] A. Yuan, Y.J. Hsiao, H.Y. Chen, H.W. Chen, C.C. Ho, Y.Y. Chen, Y.C. Liu, T.H. Hong, S.L. Yu, J.J. Chen, P.C. Yang, Opposite effects of M1 and M2 macrophage subtypes on lung cancer progression, Sci. Rep. 5 (2015) 14273.
[6] F. Pantano, P. Berti, F.M. Guida, G. Perrone, B. Vincenzi, M.M. Amato, D. Righi, E. Dell'aquila, F. Graziano, V. Catalano, M. Caricato, S. Rizzo, A.O. Muda, A. Russo, G. Tonini, D. Santini, The role of macrophages polarization in predicting prognosis of radically resected gastric cancer patients, J. Cell Mol. Med. 17 (2013) 1415–1421.
[7] R.Z. Panni, D.C. Linehan, D.G. Denardo, Targeting tumor-infiltrating macrophages to combat cancer, Immunotherapy 5 (2013) 1075–1087.
[8] J.M. Brown, L. Recht, S. Strober, The promise of targeting macrophages in cancer therapy, Clin. Cancer Res. 23 (2017) 3241–3250.
[9] G. Genard, S. Lucas, C. Michiels, Reprogramming of tumor-associated macrophages with anticancer therapies: radiotherapy versus chemo- and immunotherapies, Front. Immunol. 8 (2017) 828.
[10] O.W. Yeung, C.M. Lo, C.C. Ling, X. Qi, W. Geng, C.X. Li, K.T. Ng, S.J. Forbes, X.Y. Guan, R.T. Poon, S.T. Fan, K. Man, Alternatively activated (M2) macrophages promote tumour growth and invasiveness in hepatocellular carcinoma, J. Hepatol. 62 (2015) 607–616.
[11] A.D. Guerra, O.W.H. Yeung, X. Qi, W.J. Kao, K. Man, The anti-tumor effects of M1 macrophage-loaded poly (ethylene glycol) and gelatin-based hydrogels on hepatocellular carcinoma, Theranostics 7 (2017) 3732–3744.
[12] A.M. Georgoudaki, K.E. Prokopec, V.F. Boura, E. Hellqvist, S. Sohn, J. Ostling, R. Dahan, R.A. Harris, M. Rantalainen, D. Klevebring, M. Sund, S.E. Brage, J. Fuxe, C. Rolny, F. Li, J.V. Ravetch, M.C. Karlsson, Reprogramming tumor-associated macrophages by antibody targeting inhibits cancer progression and metastasis, Cell Rep. 15 (2016) 2000–2011.
[13] Z.G. Fridlender, A. Jassar, I. Mishalian, L.C. Wang, V. Kapoor, G. Cheng, J. Sun, S. Singhal, L. Levy, S.M. Albelda, Using macrophage activation to augment immunotherapy of established tumours, Br. J. Canc. 108 (2013) 1288–1297.
[14] S.P. Arlauckas, C.S. Garris, R.H. Kohler, M. Kitaoka, M.F. Cuccarese, K.S. Yang, M.A. Miller, J.C. Carlson, G.J. Freeman, R.M. Anthony, R. Weissleder, M.J. Pittet, In vivo imaging reveals a tumor-associated macrophage-mediated resistance pathway in anti-PD-1 therapy, Sci. Transl. Med. 9 (2017).
[15] O. Helm, J. Held-Feindt, E. Grage-Griebenow, N. Reiling, H. Ungefroren, I. Vogel, U. Kruger, T. Becker, M. Ebsen, C. Rocken, D. Kabelitz, H. Schafer, S. Sebens, Tumor-associated macrophages exhibit pro- and anti-inflammatory properties by which they impact on pancreatic tumorigenesis, Int. J. Cancer 135 (2014) 843–861.
[16] O. Helm, R. Mennrich, D. Petrick, L. Goebel, S. Freitag-Wolf, C. Roder, H. Kalthoff, C. Rocken, B. Sipos, D. Kabelitz, H. Schafer, H.H. Oberg, D. Wesch, S. Sebens, Comparative characterization of stroma cells and ductal epithelium in chronic pancreatitis and pancreatic ductal adenocarcinoma, PLoS One 9 (2014) e94357.
[17] S. Hartmann, T. Tousseyn, C. Doring, P. Fluchter, H. Hackstein, A. Herreman, M. Ponzoni, C. De Wolf-Peeters, F. Facchetti, R.D. Gascoyne, R. Kuppers, C. Steidl, M.L. Hansmann, Macrophages in T cell/histiocyte rich large B cell lymphoma strongly express metal-binding proteins and show a bi-activated phenotype, Int. J. Cancer 133 (2013) 2609–2618.
[18] S. Reinartz, T. Schumann, F. Finkernagel, A. Wortmann, J.M. Jansen, W. Meissner, M. Krause, A.M. Schworer, U. Wagner, S. Muller-Brusselbach, R. Muller, Mixed-polarization phenotype of ascites-associated macrophages in human ovarian carcinoma: correlation of CD163 expression, cytokine levels and early relapse, Int. J. Cancer 134 (2014) 32–42.
[19] U. Cho, B. Kim, S. Kim, Y. Han, Y.S. Song, Pro-inflammatory M1 macrophage enhances metastatic potential of ovarian cancer cells through NF-kappaB activation, Mol. Carcinog. 57 (2018) 235–242.
[20] T. Reya, S.J. Morrison, M.F. Clarke, I.L. Weissman, Stem cells, cancer, and cancer stem cells, Nature 414 (2001) 105–111.
[21] P.B. Gupta, C.M. Fillmore, G. Jiang, S.D. Shapira, K. Tao, C. Kuperwasser,

E.S. Lander, Stochastic state transitions give rise to phenotypic equilibrium in populations of cancer cells, Cell 146 (2011) 633–644.
[22] D. Iliopoulos, H.A. Hirsch, G. Wang, K. Struhl, Inducible formation of breast cancer stem cells and their dynamic equilibrium with non-stem cancer cells via IL6 secretion, Proc. Natl. Acad. Sci. U. S. A. 108 (2011) 1397–1402.
[23] D.E. Gyorki, M.L. Asselin-Labat, N. Van Rooijen, G.J. Lindeman, J.E. Visvader, Resident macrophages influence stem cell activity in the mammary gland, Breast Cancer Res. 11 (2009) R62.
[24] Q.M. Fan, Y.Y. Jing, G.F. Yu, X.R. Kou, F. Ye, L. Gao, R. Li, Q.D. Zhao, Y. Yang, Z.H. Lu, L.X. Wei, Tumor-associated macrophages promote cancer stem cell-like properties via transforming growth factor-beta1-induced epithelial-mesenchymal transition in hepatocellular carcinoma, Cancer Lett. 352 (2014) 160–168.
[25] J. Yang, D. Liao, C. Chen, Y. Liu, T.H. Chuang, R. Xiang, D. Markowitz, R.A. Reisfeld, Y. Luo, Tumor-associated macrophages regulate murine breast cancer stem cells through a novel paracrine EGFR/Stat3/Sox-2 signaling pathway, Stem Cell. 31 (2013) 248–258.
[26] L. Guo, C. Chen, M. Shi, F. Wang, X. Chen, D. Diao, M. Hu, M. Yu, L. Qian, N. Guo, Stat3-coordinated Lin-28-let-7-HMGA2 and miR-200-ZEB1 circuits initiate and maintain oncostatin M-driven epithelial-mesenchymal transition, Oncogene 32 (2013) 5272–5282.
[27] Z. Yang, L. Guo, D. Liu, L. Sun, H. Chen, Q. Deng, Y. Liu, M. Yu, Y. Ma, N. Guo, M. Shi, Acquisition of resistance to trastuzumab in gastric cancer cells is associated with activation of IL-6/STAT3/Jagged-1/Notch positive feedback loop, Oncotarget 6 (2015) 5072–5087.
[28] J.W. Tjiu, J.S. Chen, C.T. Shun, S.J. Lin, Y.H. Liao, C.Y. Chu, T.F. Tsai, H.C. Chiu, Y.S. Dai, H. Inoue, P.C. Yang, M.L. Kuo, S.H. Jee, Tumor-associated macrophage-induced invasion and angiogenesis of human basal cell carcinoma cells by cyclooxygenase-2 induction, J. Investig. Dermatol. 129 (2009) 1016–1025.
[29] C. Fillmore, C. Kuperwasser, Human breast cancer stem cell markers CD44 and CD24: enriching for cells with functional properties in mice or in man? Breast Cancer Res. 9 (2007) 303.
[30] C. Ginestier, M.H. Hur, E. Charafe-Jauffret, F. Monville, J. Dutcher, M. Brown, J. Jacquemier, P. Viens, C.G. Kleer, S. Liu, A. Schott, D. Hayes, D. Birnbaum, M.S. Wicha, G. Dontu, ALDH1 is a marker of normal and malignant human mammary stem cells and a predictor of poor clinical outcome, Cell Stem Cell 1 (2007) 555–567.
[31] X. Li, M.T. Lewis, J. Huang, C. Gutierrez, C.K. Osborne, M.F. Wu, S.G. Hilsenbeck, A. Pavlick, X. Zhang, G.C. Chamness, H. Wong, J. Rosen, J.C. Chang, Intrinsic resistance of tumorigenic breast cancer cells to chemotherapy, J. Natl. Cancer Inst. 100 (2008) 672–679.
[32] A.K. Bonde, V. Tischler, S. Kumar, A. Soltermann, R.A. Schwendener, Intratumoral macrophages contribute to epithelial-mesenchymal transition in solid tumors, BMC Canc. 12 (2012) 35.
[33] S.A. Mani, W. Guo, M.J. Liao, E.N. Eaton, A. Ayyanan, A.Y. Zhou, M. Brooks, F. Reinhard, C.C. Zhang, M. Shipitsin, L.L. Campbell, K. Polyak, C. Brisken, J. Yang, R.A. Weinberg, The epithelial-mesenchymal transition generates cells with properties of stem cells, Cell 133 (2008) 704–715.
[34] H. Lu, K.R. Clauser, W.L. Tam, J. Frose, X. Ye, E.N. Eaton, F. Reinhardt, V.S. Donnenberg, R. Bhargava, S.A. Carr, R.A. Weinberg, A breast cancer stem cell niche supported by juxtacrine signalling from monocytes and macrophages, Nat. Cell Biol. 16 (2014) 1105–1117.
[35] R. Kalluri, R.A. Weinberg, The basics of epithelial-mesenchymal transition, J. Clin. Investig. 119 (2009) 1420–1428.
[36] J. Bollrath, F.R. Greten, IKK/NF-kappaB and STAT3 pathways: central signalling hubs in inflammation-mediated tumour promotion and metastasis, EMBO Rep. 10 (2009) 1314–1319.
[37] M.R. Copley, S. Babovic, C. Benz, D.J. Knapp, P.A. Beer, D.G. Kent, S. Wohrer, D.Q. Treloar, C. Day, K. Rowe, H. Mader, F. Kuchenbauer, R.K. Humphries, C.J. Eaves, The Lin28b-let-7-Hmga2 axis determines the higher self-renewal potential of fetal haematopoietic stem cells, Nat. Cell Biol. 15 (2013) 916–925.
[38] S.K. Biswas, A. Sica, C.E. Lewis, Plasticity of macrophage function during tumor progression: regulation by distinct molecular mechanisms, J. Immunol. 180 (2008) 2011–2017.
[39] D.M. Kuang, Y. Wu, N. Chen, J. Cheng, S.M. Zhuang, L. Zheng, Tumor-derived hyaluronan induces formation of immunosuppressive macrophages through transient early activation of monocytes, Blood 110 (2007) 587–595.
[40] J. Yu, M.A. Vodyanik, K. Smuga-Otto, J. Antosiewicz-Bourget, J.L. Frane, S. Tian, J. Nie, G.A. Jonsdottir, V. Ruotti, R. Stewart, Ii Slukvin, J.A. Thomson, Induced pluripotent stem cell lines derived from human somatic cells, Science 318 (2007) 1917–1920.
[41] B. Hamilton, Q. Feng, M. Ye, G.G. Welstead, Generation of induced pluripotent stem cells by reprogramming mouse embryonic fibroblasts with a four transcription factor, doxycycline inducible lentiviral transduction system, JoVE 33 (2009).
[42] C.D. Mills, L.L. Lenz, R.A. Harris, A breakthrough: macrophage-directed cancer immunotherapy, Cancer Res. 76 (2016) 513–516.
[43] D.M. Kuang, C. Peng, Q. Zhao, Y. Wu, L.Y. Zhu, J. Wang, X.Y. Yin, L. Li, L. Zheng, Tumor-activated monocytes promote expansion of IL-17-producing CD8+ T cells in hepatocellular carcinoma patients, J. Immunol. 185 (2010) 1544–1549.
[44] M. Quiding-Jarbrink, S. Raghavan, M. Sundquist, Enhanced M1 macrophage polarization in human helicobacter pylori-associated atrophic gastritis and in vaccinated mice, PLoS One 5 (2010) e15018.
[45] H. Sugai, K. Kono, A. Takahashi, F. Ichihara, H. Kawaida, H. Fujii, Y. Matsumoto, Characteristic alteration of monocytes with increased intracellular IL-10 and IL-12 in patients with advanced-stage gastric cancer, J. Surg. Res. 116 (2004) 277–287.
[46] T. Hagemann, J. Wilson, F. Burke, H. Kulbe, N.F. Li, A. Pluddemann, K. Charles, S. Gordon, F.R. Balkwill, Ovarian cancer cells polarize macrophages toward a tumor-associated phenotype, J. Immunol. 176 (2006) 5023–5032.
[47] G.T. Bardi, M.A. Smith, J.L. Hood, Melanoma exosomes promote mixed M1 and M2 macrophage polarization, Cytokine 105 (2018) 63–72.
[48] S. Brabletz, T. Brabletz, The ZEB/miR-200 feedback loop–a motor of cellular plasticity in development and cancer? EMBO Rep. 11 (2010) 670–677.
[49] W. Guo, Z. Keckesova, J.L. Donaher, T. Shibue, V. Tischler, F. Reinhardt, S. Itzkovitz, A. Noske, U. Zurrer-Hardi, G. Bell, W.L. Tam, S.A. Mani, A. Van Oudenaarden, R.A. Weinberg, Slug and Sox9 cooperatively determine the mammary stem cell state, Cell 148 (2012) 1015–1028.
[50] Y. Kong, Y. Peng, Y. Liu, H. Xin, X. Zhan, W. Tan, Twist1 and Snail link Hedgehog signaling to tumor-initiating cell-like properties and acquired chemoresistance independently of ABC transporters, Stem Cell. 33 (2015) 1063–1074.
[51] C.S. Chien, M.L. Wang, P.Y. Chu, Y.L. Chang, W.H. Liu, C.C. Yu, Y.T. Lan, P.I. Huang, Y.Y. Lee, Y.W. Chen, W.L. Lo, S.H. Chiou, Lin28B/Let-7 regulates expression of Oct4 and Sox2 and reprograms oral squamous cell carcinoma cells to a stem-like state, Cancer Res. 75 (2015) 2553–2565.
[52] N. Shyh-Chang, G.Q. Daley, Lin28: primal regulator of growth and metabolism in stem cells, Cell Stem Cell 12 (2013) 395–406.
[53] E. Piskounova, C. Polytarchou, J.E. Thornton, R.J. Lapierre, C. Pothoulakis, J.P. Hagan, D. Iliopoulos, R.I. Gregory, Lin28A and Lin28B inhibit let-7 microRNA biogenesis by distinct mechanisms, Cell 147 (2011) 1066–1079.
[54] F. Yu, H. Yao, P. Zhu, X. Zhang, Q. Pan, C. Gong, Y. Huang, X. Hu, F. Su, J. Lieberman, E. Song, let-7 regulates self renewal and tumorigenicity of breast cancer cells, Cell 131 (2007) 1109–1123.
[55] J. Nishino, I. Kim, K. Chada, S.J. Morrison, Hmga2 promotes neural stem cell self-renewal in young but not old mice by reducing p16Ink4a and p19Arf Expression, Cell 135 (2008) 227–239.
[56] O. Li, D. Vasudevan, C.A. Davey, P. Droge, High-level expression of DNA architectural factor HMGA2 and its association with nucleosomes in human embryonic stem cells, Genesis 44 (2006) 523–529.
[57] G.Y. Chiou, C.S. Chien, M.L. Wang, M.T. Chen, Y.P. Yang, Y.L. Yu, Y. Chien, Y.C. Chang, C.C. Shen, C.C. Chio, K.H. Lu, H.I. Ma, K.H. Chen, D.M. Liu, S.A. Miller, Y.W. Chen, P.I. Huang, Y.H. Shih, M.C. Hung, S.H. Chiou, Epigenetic regulation of the miR142-3p/interleukin-6 circuit in glioblastoma, Mol. Cell 52 (2013) 693–706.
[58] K. Movahedi, S. Schoonooghe, D. Laoui, I. Houbracken, W. Waelput, K. Breckpot, L. Bouwens, T. Lahoutte, P. De Baetselier, G. Raes, N. Devoogdt, J.A. Van Ginderachter, Nanobody-based targeting of the macrophage mannose receptor for effective in vivo imaging of tumor-associated macrophages, Cancer Res. 72 (2012) 4165–4177.
[59] S.M. Pyonteck, B.B. Gadea, H.W. Wang, V. Gocheva, K.E. Hunter, L.H. Tang, J.A. Joyce, Deficiency of the macrophage growth factor CSF-1 disrupts pancreatic neuroendocrine tumor development, Oncogene 31 (2012) 1459–1467.
[60] M. Smahel, M. Duskova, I. Polakova, J. Musil, Enhancement of DNA vaccine potency against legumain, J. Immunother. 37 (2014) 293–303.
[61] A. Sica, A. Mantovani, Macrophage plasticity and polarization: in vivo veritas, J. Clin. Investig. 122 (2012) 787–795.
[62] T. Seya, H. Shime, M. Matsumoto, TAMable tumor-associated macrophages in response to innate RNA sensing, OncoImmunology 1 (2012) 1000–1001.
[63] L. Yang, F. Wang, L. Wang, L. Huang, J. Wang, B. Zhang, Y. Zhang, CD163+ tumor-associated macrophage is a prognostic biomarker and is associated with therapeutic effect on malignant pleural effusion of lung cancer patients, Oncotarget 6 (2015) 10592–10603.
[64] M. Song, T. Liu, C. Shi, X. Zhang, X. Chen, Bioconjugated manganese dioxide nanoparticles enhance chemotherapy response by priming tumor-associated macrophages toward M1-like phenotype and attenuating tumor hypoxia, ACS Nano 10 (2016) 633–647.
[65] G.C. Chan, W.K. Chan, D.M. Sze, The effects of beta-glucan on human immune and cancer cells, J. Hematol. Oncol. 2 (2009) 25.
[66] O. Helm, J. Held-Feindt, H. Schafer, S. Sebens, M1 and M2: there is no "good" and "bad"-How macrophages promote malignancy-associated features in tumorigenesis, OncoImmunology 3 (2014) e946818.
[67] G.K. Chimal-Ramirez, N.A. Espinoza-Sanchez, L. Chavez-Sanchez, L. Arriaga-Pizano, E.M. Fuentes-Panana, Monocyte differentiation towards protumor activity does not correlate with M1 or M2 phenotypes, J. Immunol. Res. 2016 (2016) 6031486.